BOLLETTINO DI GEOFISICA TEORICA ED APPLICATA VOL. 40, N. 1, pp. 1-18; MARCH 1999

The best isotropic approximation of an anisotropic Hooke's law

F. CAVALLINI

Osservatorio Geofisico Sperimentale, Trieste, Italy

(Received June 26, 1998; accepted March 9, 1999)

Abstract. What is the best isotropic approximation of an anisotropic stiffness tensor? How can we quantify isotropy with a single numerical index? This article gives a precise meaning to these questions by introducing an orthogonal projector from the stiffness tensors space onto the isotropic tensors subspace. Moreover, explicit expressions are derived for the Lamé parameters of this approximation, when the data are either in coordinate-free form or in Voigt's notation. Thus it is possible to unravel the effect of anisotropy on time-harmonic plane wave propagation. Detailed computations are shown in the case of ANNIE shales, which are transversely isotropic, by way of example. Finally, the isotropic approximations of 44 shales are computed, with the result that the anisotropy index is less than ten percent for just five of them. Potential applications of this approach to rock physics, seismic exploration, reservoir engineering, and seismology are briefly outlined.

1. Introduction

. . . ridicules calculs de matrices.
J. Dieudonné

Anisotropy is, nowadays, a well established branch of exploration geophysics (Fjær et al., 1996). There are two main reasons for this. Firstly, many rocks of interest to the oil industry are intrinsically anisotropic, as in the case - for example - of shales, which are transversely isotropic (Schoenberg, 1996). Secondly, the theory of the equivalent medium shows that a finely layered formation composed of different homogeneous isotropic layers is equivalent - from the point of view of seismic exploration - to a homogeneous anisotropic formation, provided that the wavelength of the probing wave is much longer than the thickness of the layers (e.g., Carcione, 1992).

Moreover, investigating seismic anisotropy is considered one of the most effective methods for obtaining information on the orientation of crystals and on the different types of fine structu-

Corresponding author: F. Cavallini; Osservatorio Geofisico Sperimentale, P.O. Box 2011, 34016 Opicina, Italy; tel. +39 040 2140 306; fax +39 040 327521; e-mail: fcavallini@ogs.trieste.it

res under the action of large-scale geodynamical processes within the Earth's deep interior, with obvious impact on tectonophysics, seismology and geology (Babuska and Cara, 1991). Other background material on anisotropy for geophysicists is contained, for example, in Crampin (1981) and Helbig (1994).

Although the theory of anisotropic elasticity was already well developed in the 19 th century (e.g., Thomson, 1856, and Curie, 1884), many geophysicists are still reluctant to include anisotropy in their computer models of seismic wave propagation. Besides the intricacies inherent in the mathematical formalism of anisotropy, this attitude is due to the challenging increase in computational complexity that accompanies the "jump" from isotropy to anisotropy. Indeed, an isotropic rheology is characterized by just two space-dependent parameters, whereas a general (i.e., triclinic) anisotropic medium has 21 independent elastic moduli; and five moduli are required by transversely isotropic media, which constitute the simplest class of general geophysical interest. Thus, in a numerical model with N nodes, the increase in the number of memory positions required to store the elastic parameters is from $2N$ (isotropic case) to $21N$ (triclinic case), where N is usually a very large number, especially in the case of 3-D simulations. Even subtler and more serious problems arise in connection with inverse modelling (e.g., traveltime tomography). Indeed, inverse problems are intrinsically ill-posed and, as such, suffer from nonuniqueness, instability, ill-conditioning, etc.; and - in general - these difficulties dramatically increase with the number of parameters to be identified.

At this point it appears that a reasonable approach to any elastic modelling might be the following: firstly, to develop a rough anisotropic model; secondly, to consider the isotropic model nearest to the isotropic one; thirdly, to compare the results obtained from each model and start tuning the anisotropic one only if the effects of anisotropy are of primary importance, otherwise choose the cheaper and more robust isotropic model.

This discussion should have clarified the geophysical relevance of the following problem: what is the best isotropic approximation of an anisotropic stiffness tensor? Fedorov (1968) has given a solution to this problem via an *analytic* approach: the derivatives of a suitable anisotropy function with respect to the elastic moduli are put equal to zero. Arts (1993) has generalized this approach to lower material symmetries.

The principal aim of this article is to obtain Fedorov's isotropic results - and more - by using a *geometric* approach: an inner product is naturally defined over the space of stiffness operators, and an orthogonal projector onto the isotropic subspace is introduced. Whereas Fedorov uses a four-subscript tensor notation, here we shall take advantage of a coordinate-free notation, which, as such, shows the physical contents of the procedure and of the results more clearly. However, the *de facto* standard notation in anisotropic studies is Voigt's condensed notation, and therefore we shall formulate the main results in Voigt's notation also. As the link between intrinsic and Voigt's notation is not immediate, we shall also use as an intermediate step in the next section a third notation based on canonical bases. Appendix A contains a brief review of the main concepts in linear and tensor algebra used in this work, and should be read before or in parallel with Section 2. Section 3 shows several applications of these formulae to actual rheological models of geophysical interest. The emphasis is on shales, because of their importance in the oil industry. Symbolic formulae are obtained for the ANNIE model of shale, which uses only three parame-

ters instead of the five moduli needed by a transversely isotropic constitutive law (Schoenberg et al., 1996). Moreover, the anisotropy index introduced in Section 2 is computed for 44 shales using experimental data from the relevant literature, with the aim of ascertaining the adequacy/inadequacy of the approximate isotropic model for shales.

2. Theory

2.1. Coordinate-free results

Referring to Appendix 1 for mathematical notations and background material, we start here by considering the coordinate-free formulation of generalized Hooke's law for isotropic materials (e.g., Gurtin, 1981), in which stress is expressed as

$$C_0\,[\mathbf{E}] = \lambda\,\mathrm{trc}[\mathbf{E}]\,\mathbf{I} + 2\,\mu\,\mathbf{E}, \tag{1}$$

where λ and μ are Lamé parameters, $\mathbf{I}$ is the 3×3 identity matrix, and $\mathbf{E}$ represents strain. Writing I for the identity map over the 6-dimensional space Sym of 3×3 symmetric matrices, and introducing the operator $J \equiv \mathbf{I} \otimes \mathbf{I}$, Hooke's law (1) may be written in the more compact form

$$C_0 = \lambda\, J + 2\,\mu I. \tag{2}$$

This formulation of isotropic Hooke's law will lead us quickly and directly to the expression of the best isotropic approximation for an anisotropic stiffness operator. Indeed, operators I and J may be thought of as vectors belonging to the space L_S [Sym] of linear symmetric operators over Sym; therefore, because of (2), the space Iso of isotropic stiffness operators is constituted by all the linear combinations of I and J. In symbols, we have

$$\mathrm{Iso} = \mathrm{span}\{I, J\}. \tag{3}$$

By (50), the projector on this subspace is given by

$$P_{\mathrm{Iso}} = \frac{1}{I^2 J^2 - (I \cdot J)^2}\quad \left(J^2 I \otimes I + I^2 J \otimes J - 2(I \cdot J)\ \mathrm{sym}\,[I \otimes J]\right) \tag{4}$$

Straightforward coordinate-free computations show that

$$I^2 = 6, \qquad I \cdot J = 3, \qquad J^2 = 9 \tag{5}$$

Thus, P_{Iso} simplifies into

$$P_{\text{Iso}} = \frac{1}{15}\left(3I \otimes I + 2J \otimes J - 2\text{sym}[I \otimes J]\right) \tag{6}$$

and hence the best isotropic approximation of an anisotropic stiffness operator C (assumed to be symmetric and positive definite because of thermodynamic constraints) is $C_0 = P_{\text{Iso}}\, C$, i.e.,

$$C_0 = \lambda_0 J + 2\mu_0 I, \tag{7}$$

where

$$\lambda_0 \equiv \frac{1}{15}(2J \cdot C - I \cdot C) = \frac{1}{15}\left(2\text{trc}[C[\mathbf{I}]] - \text{trc}[C]\right), \tag{8}$$

and

$$\mu_0 \equiv \frac{1}{30}(3I \cdot C - J \cdot C) = \frac{1}{30}\left(3\text{trc}[C] - \text{trc}[C[\mathbf{I}]]\right), \tag{9}$$

may be called the *approximate Lamé parameters*. The *anisotropy index*

$$I_A \equiv \frac{\|C - C_0\|}{\|C\|} = \sqrt{1 - \frac{\|C_0\|^2}{\|C\|^2}} \tag{10}$$

is the ratio of the distance between C and Iso to the length of C; as such, it is really a measure of the anisotropy of C. The second equality in formula (10) is an obvious consequence of the theorem of Pythagoras. Indeed, C_0 is the orthogonal projection of the elasticity tensor C onto the isotropic subspace Iso; then, the theorem of Pythagoras (which holds in any Hilbert space) yields $||C||^2 = ||C_0||^2 + ||C - C_0||^2$. This fact is illustrated heuristically in Fig. 1. Hence, one can readily show that $||C_0|| \le ||C||$ (the hypotenuse is the longest side); therefore $0 \le I_A \le 1$. Actually, the above assumptions rule out the case $I_A = 1$. Finally, we note that the expression $||C_0||^2$, which appears in (10), is related to the approximate Lame parameters via

$$\|C_0\|^2 = 9\lambda_0^2 + 24\mu_0^2 + 12\lambda_0\mu_0. \tag{11}$$

2.2. Canonical bases

Using the canonical orthonormal basis in $\Re^3$

$$\hat{\mathbf{e}}_1=\{1,0,0\}, \qquad \hat{\mathbf{e}}_2=\{0,1,0\}, \qquad \hat{\mathbf{e}}_3=\{0,0,1\}, \tag{12}$$

we may construct the following orthonormal basis in Sym:

$$\hat{\mathbf{E}}_1=\hat{\mathbf{e}}_1\otimes\hat{\mathbf{e}}_1 \qquad \hat{\mathbf{E}}_4=\left(\hat{\mathbf{e}}_2\otimes\hat{\mathbf{e}}_3+\hat{\mathbf{e}}_3\otimes\hat{\mathbf{e}}_2\right)/\sqrt{2}, \tag{13}$$

$$\hat{\mathbf{E}}_2=\hat{\mathbf{e}}_2\otimes\hat{\mathbf{e}}_2 \qquad \hat{\mathbf{E}}_5=\left(\hat{\mathbf{e}}_1\otimes\hat{\mathbf{e}}_3+\hat{\mathbf{e}}_3\otimes\hat{\mathbf{e}}_1\right)/\sqrt{2}, \tag{14}$$

$$\hat{\mathbf{E}}_3=\hat{\mathbf{e}}_3\otimes\hat{\mathbf{e}}_3 \qquad \hat{\mathbf{E}}_6=\left(\hat{\mathbf{e}}_1\otimes\hat{\mathbf{e}}_2+\hat{\mathbf{e}}_2\otimes\hat{\mathbf{e}}_1\right)/\sqrt{2}, \tag{15}$$

and the following identities

$$\mathrm{trc}\left[\hat{\mathbf{E}}_I\right]=\begin{cases}1 & \text{if } I\le 3\\ 0 & \text{if } 3<I\end{cases} \tag{16}$$

$$\mathbf{I}=\sum_{i=1}^{3}\hat{\mathbf{E}}_i \tag{17}$$

hold because of the orthonormality of basis (12). Further, an orthonormal basis in L[Sym] may be introduced through

$$\hat{\varepsilon}_{IJ}=\hat{\mathbf{E}}_I\otimes\hat{\mathbf{E}}_J, \qquad I,J=1,...,6 \tag{18}$$

Then, the identity map over Sym (which belongs to L[Sym] and L_S [Sym] as well) is given by

$$I=\sum_{I=1}^{6}\hat{\varepsilon}_{II}, \tag{19}$$

and the generic stiffness operator may be expanded as

$$C=\sum_{I,J=1}^{6}\hat{c}_{IJ}\hat{\varepsilon}_{IJ} \tag{20}$$

where the coefficients in the expansion are

$$\hat{c}_{IJ}=\hat{\mathbf{E}}_I\cdot C\left[\hat{\mathbf{E}}_J\right]. \tag{21}$$

Therefore

$$\mathrm{trc}[C]=\sum_{I=1}^{6}\hat{c}_{II}, \qquad \mathrm{trc}\left[C[\mathbf{I}]\right]=\sum_{i,j=1}^{3}\hat{c}_{ij} \tag{22}$$

and hence the approximate Lamé parameters (8) and (9) are expressed in canonical coordinates $\hat{c}_{IJ}$ as

$$\lambda_0 = \frac{1}{15}\left(\hat{c}_{11} + \hat{c}_{22} + \hat{c}_{33} - \left(\hat{c}_{44} + \hat{c}_{55} + \hat{c}_{66}\right) + 4\left(\hat{c}_{12} + \hat{c}_{13} + \hat{c}_{23}\right)\right) \tag{23}$$

$$\mu_0 = \frac{1}{15}\left(\hat{c}_{11} + \hat{c}_{22} + \hat{c}_{33} + \frac{3}{2}\left(\hat{c}_{44} + \hat{c}_{55} + \hat{c}_{66}\right) - \left(\hat{c}_{12} + \hat{c}_{13} + \hat{c}_{23}\right)\right) \tag{24}$$

Finally, we note that

$$\|C\|^2 = \sum_{I,J=1}^{6} \hat{c}_{IJ}^2, \tag{25}$$

so that the anisotropy index I_A can be computed in terms of canonical coordinates using (10), (11) and (23)-(25).

2.3. Voigt's notation

The Voigt's notation is important because it has become the standard in anisotropic elasticity. Nevertheless, it must be noted that, from the point of view of abstract algebra, it is not the most natural or most convenient notation: as such, a careless use of this notation may lead to serious errors, as some examples discussed in Appendix 3 will show.

In Voigt's notation, the stiffness operator is represented by a 6×6 symmetric matrix whose entries c_{IJ} are related to the canonical elements $\hat{c}_{IJ}$ through the following identities (Mehrabadi and Cowin, 1990):

$$\begin{aligned} &\hat{c}_{ij} = c_{ij} && \text{for } i,j = 1,2,3; \\ &\hat{c}_{IJ} = 2c_{IJ} && \text{for } I,J = 4,5,6; \\ &\hat{c}_{iJ} = \sqrt{2}c_{iJ} && \text{for } i = 1,2,3;\ J = 4,5,6 \end{aligned} \tag{26}$$

Therefore, equations (23) and (24) yield the approximate Lamé parameters in the form

$$\lambda_0 = \frac{1}{15}\left(c_{11} + c_{22} + c_{33} - 2\left(c_{44} + c_{55} + c_{66}\right) + 4\left(c_{12} + c_{13} + c_{23}\right)\right), \tag{27}$$

$$\mu_0 = \frac{1}{15}\left(c_{11} + c_{22} + c_{33} + 3\left(c_{44} + c_{55} + c_{66}\right) - \left(c_{12} + c_{13} + c_{23}\right)\right). \tag{28}$$

Likewise, from (25) we obtain

$$\|C\|^2 = \sum_{i,j=1}^{3} {c_{ij}}^2 + 4\sum_{I,J=4}^{6} {c_{IJ}}^2 + 4\sum_{i=1}^{3}\sum_{J=4}^{6} {c_{iJ}}^2, \tag{29}$$

so that the anisotropy index I_A can be computed in Voigt's notation using (10), (11) and (27)-(29).

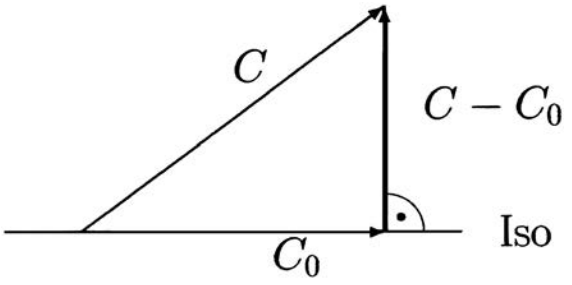

Fig. 1. - The anisotropic elasticity tensor C is projected orthogonally onto the isotropic subspace Iso, yielding the best isotropic approximation C_0 .

3. Examples

3.1. Isotropic symmetry

COORDINATE-FREE NOTATION. - Because of (8) and (9), an isotropic elastic tensor given by equation (1) has the approximate Lamé parameters

$$\lambda_0 = \lambda, \qquad \mu_0 = \mu \tag{30}$$

as expected, because

$$\mathrm{trc}\left[C_0[\mathbf{I}]\right] = 3(3\lambda + 2\mu) \tag{31}$$

and, from equations (5),

$$\mathrm{trc}\left[C_0\right] = 3(\lambda + 4\mu) \tag{32}$$

In other words, we have proved that the approximate Lamé parameters coincide, in the isotropic case, with the usual Lamé parameters.

VOIGT'S NOTATION. - In Voigt's notation, the isotropic stiffness operator (1) is represented by a 6×6 matrix whose elements are (Auld, 1990)

$$\begin{aligned} c_{ii} &= \lambda + 2\mu \quad \text{for } i = 1,\ 2,\ 3 \\ c_{ij} &= \lambda \quad \text{for } i, j = 1,\ 2,\ 3 \quad (i \neq j) \\ c_{II} &= \mu \quad \text{for } I = 4,\ 5,\ 6 \\ c_{IJ} &= 0 \quad \text{otherwise} \end{aligned} \tag{33}$$

as can be derived from (26) using (21) and (2).

Then, (27) and (28) yield (30) again.

3.2. Transversely isotropic symmetry

GENERAL CASE. - In Voigt's notation, the stiffness matrix of a general transversely isotropic medium may be written as (Grant and West, 1965)

$$c^{\mathrm{TI}} = \begin{bmatrix} \lambda_{\|}+2\mu_{\|} & \lambda_{\|} & \lambda_{\perp} & 0 & 0 & 0 \\ \lambda_{\|} & \lambda_{\|}+2\mu_{\|} & \lambda_{\perp} & 0 & 0 & 0 \\ \lambda_{\perp} & \lambda_{\perp} & \lambda_{\perp}+2\mu_{\perp} & 0 & 0 & 0 \\ 0 & 0 & 0 & \nu & 0 & 0 \\ 0 & 0 & 0 & 0 & \nu & 0 \\ 0 & 0 & 0 & 0 & 0 & \mu_{\|} \end{bmatrix} \tag{34}$$

where the z–axis has been chosen to coincide with the symmetry axis of the material. Therefore, its generalized Lamé parameters are, from (27) and (28)

$$\lambda_0^{\mathrm{TI}} = \frac{1}{5}\left(2\lambda_{\|}+3\lambda_{\perp}\right)+\frac{2}{15}\left(\mu_{\|}+\mu_{\perp}-2\nu\right) \tag{35}$$

$$\mu_0^{\mathrm{TI}} = \frac{1}{15}\left(\lambda_{\|}-\lambda_{\perp}\right)+\frac{1}{15}\left(7\mu_{\|}+2\mu_{\perp}-6\nu\right) \tag{36}$$

Somewhat surprisingly, the parameter λ_0 also depends on $\mu_{\|}, \mu_{\perp}, \nu$ (and not only on $\lambda_{\|}$ and $\lambda_{\perp}$); similarly for μ_0.

ANNIE SHALES. - If we assume that equation (34) holds with

$$\lambda_{\|} = \lambda_{\perp} \equiv \lambda, \qquad \nu = \mu_{\perp}, \tag{37}$$

then we get

$$c^{\mathrm{ANNIE}} = \begin{bmatrix} \lambda+2\mu_{\|} & \lambda & \lambda & 0 & 0 & 0 \\ \lambda & \lambda+2\mu_{\|} & \lambda & 0 & 0 & 0 \\ \lambda & \lambda & \lambda+2\mu_{\perp} & 0 & 0 & 0 \\ 0 & 0 & 0 & \mu_{\perp} & 0 & 0 \\ 0 & 0 & 0 & 0 & \mu_{\perp} & 0 \\ 0 & 0 & 0 & 0 & 0 & \mu_{\|} \end{bmatrix} \tag{38}$$

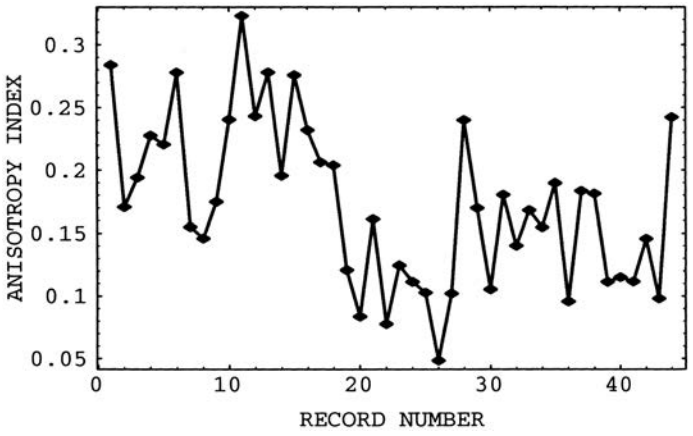

Fig. 2. - Anisotropy index I_A of 44 samples of dry shales whose elastic parameters are deduced from the measured data listed in Vernik and Liu (1997). The minimum and maximum values of the anisotropy index are 0.048 and 0.323, respectively; the median is 0.17.

which is, by definition, the stiffness matrix of the so-called ANNIE rheological model of shales (Schoenberg et al., 1996). Therefore, its approximate Lamé parameters are, from equations (35) and (36),

$$\lambda_0^{\text{ANNIE}} = \lambda + \frac{2}{15}(\mu_{\parallel} - \mu_{\perp}), \qquad \mu_0^{\text{ANNIE}} = \frac{1}{15}(7\mu_{\parallel} - 8\mu_{\perp}) \tag{39}$$

From the previous equations it appears that, contrary to the general transversely isotropic case (36), the shear approximate Lamé parameter μ_0^{ANNIE} is independent from the compressional Lamé parameter λ.

EXPERIMENTAL DATA. - For some rocks the anisotropy index may be very small, and then their rheological behaviour may be adequately simulated using their approximate Lamé parameters. This is the case, for example, of dry Tennessee marble (Thill et al., 1973), for which the anisotropy index may be as small as 0.02, in correspondence to a transversely isotropic Voigt matrix with stiffnesses

$$c_{11} = 79 \qquad c_{13} = 15 \qquad c_{33} = 76 \qquad c_{44} = 30 \qquad c_{66} = 31.5 \tag{40}$$

where physical units are GPa. We shall now see that, in general, things are not so simple.

Shales constitute a class of rocks of great importance for petroleum geoscience. Vernik and Liu (1997) present a compilation of physical parameters pertaining to more than sixty shales with transversely isotropic symmetry. We analyze here 44 of these data records, namely all those that

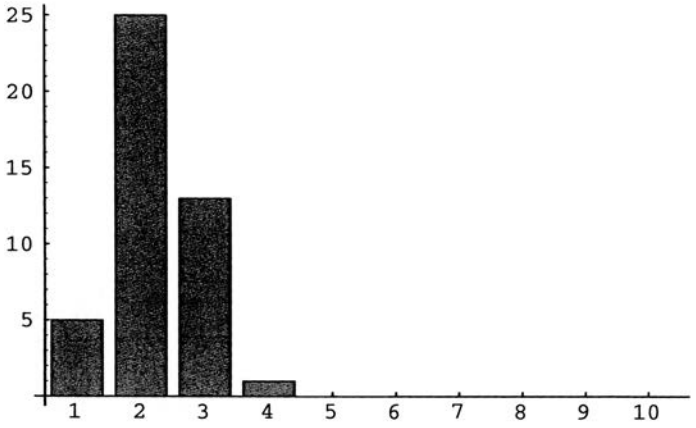

Fig. 3. - Histogram of the anisotropy index I_A for the 44 dry shales whose elastic parameters are listed in Vernik and Liu (1997). For each interval on the axis of abscissas, the number N of shales with anisotropy index lying in that interval is shown.

refer to dry samples and include the anisotropy parameter δ (Thomsen, 1986) besides density ρ, and the velocities V_P (0), V_P (90), V_S (0), V_{SH} (90) of pressure or shear ultrasonic waves propagating in a direction parallel to the axis of symmetry or perpendicular to it. Indeed from these parameters the elastic stiffnesses can be computed using the following identities:

$$c_{11} = \rho V_P(90)^2 \tag{41}$$

$$c_{33} = \rho V_P(0)^2 \tag{42}$$

$$c_{44} = \rho V_S(0)^2 \tag{43}$$

$$c_{66} = \rho V_{SH}(90)^2 \tag{44}$$

$$c_{13} = -c44 + \sqrt{(c_{33} - c_{44})(c_{33} - c_{44} + 2c_{33}\delta)} \tag{45}$$

and hence, in turn, the anisotropy index can be obtained.

Figure 2 shows the anisotropy index of these samples. This index ranges from a minimum value of 0.048 to a maximum of 0.323, and it is intuitive that while in the former case the isotropic approximation should be adequate, in the latter the rheological effects should depart substantially from the isotropic ones. A plane-wave analysis will soon confirm this view (see Figs. 5 and 6). The median of the anisotropy indexes is 0.17.

Figure 3 shows a histogram of the anisotropy index of all the shales considered in Fig. 2. There are ten frequency classes, the width of each class being 0.1. The most salient feature of this figure is that only the four lower frequency classes are nonempty: 25 out of 44 shales belong to the most populated class, having $0.1 < I_A < 0.2$, whereas the anisotropy index is less than 0.1 for only 5 shales.

Figure 4 shows a scatter plot of the approximate Lamé parameters for these shales and a

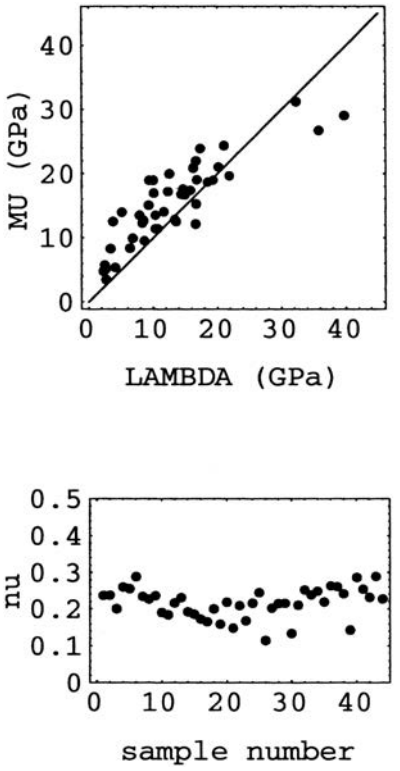

Fig. 4. - A scatter plot of the approximate Lamé parameters of the shales considered in Figs. 1 and 2 (top) is shown with the corresponding Poisson's ratio (bottom). It appears that the rheological properties of shales are only roughly approximated by a Poisson's solid, characterized by $\lambda = \mu$ and hence $\nu = 1/4$.

Cartesian plot for the corresponding Poisson's ratio. Poisson's ratio ν must fulfill the condition $-1 \leq \nu \leq 1/2$ to ensure the stability of the medium, and most materials have a positive Poisson's ratio; therefore it appears from Fig. 4 that a Poisson solid (for which $\lambda = \mu$ and hence $\nu = 1/4$) is a rather crude one-parameter approximation for the rheology of shales.

THE EFFECTS OF ANISOTROPY ON WAVE PROPAGATION. - A plane wave displacement may be written in the form

$$\mathbf{u} = u\left[\omega\left(s\hat{\mathbf{k}} \cdot \mathbf{x} - t\right)\right] \hat{\mathbf{u}}, \tag{46}$$

where s denotes slowness, while $\hat{\mathbf{k}}$ and $\hat{\mathbf{u}}$ are unit vectors called propagation direction and polarization, respectively. Such a wave may propagate in a homogeneous elastic medium if and only if the following propagation condition is fulfilled:

$$\det\left[s^2 \mathbf{A}\left[\hat{\mathbf{k}}\right] - \mathbf{I}\right] = 0 \tag{47}$$

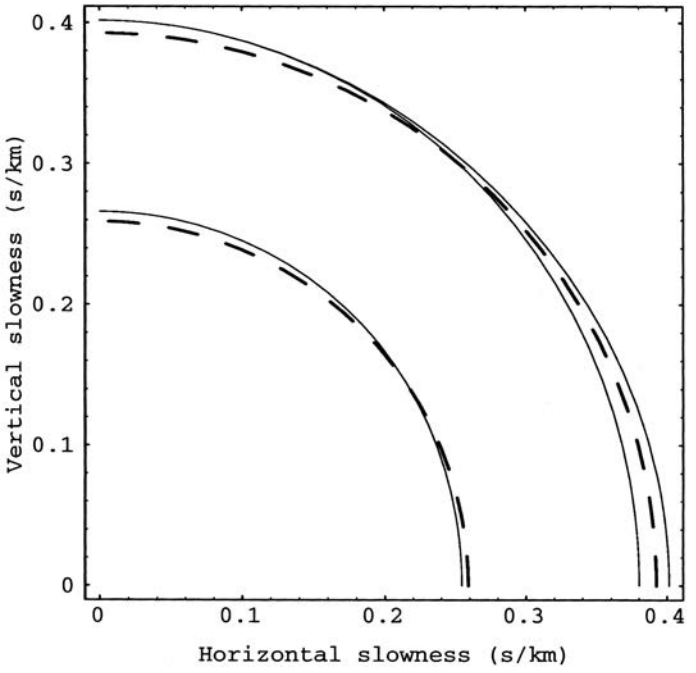

Fig. 5. - Slowness surfaces for the dry shale sample having the lowest anisotropy index among the 44 such samples considered in Vernik and Liu (1997). Solid lines (—) represent the slowness surfaces of the sample assumed as transversely isotropic, while broken lines (- -) represent the slowness surfaces of the corresponding best isotropic approximation, which in this case results reasonable.

where the acoustic tensor $\mathbf{A}[\hat{\mathbf{k}}]$ is defined by

$$\mathbf{A}\left[\hat{\mathbf{k}}\right]\mathbf{a} = \frac{1}{\rho} C\left[\mathrm{sym}\left[\hat{\mathbf{k}} \otimes \mathbf{a}\right]\right]\hat{\mathbf{k}} \tag{48}$$

for any three-dimensional vector **a** (Gurtin, 1981). The left-hand side of Christoffel's equation (47) is a third-order polynomial in s^2 ; hence, for fixed $\hat{\mathbf{k}}$, we can solve for s^2 obtaining one to three values, which are all positive because of the assumed stability of the medium. The spherical polar plot of the multi-valued function $\sqrt{s^2}$ is called *slowness surface* and is often used as a pictorial tool for representing the plane-wave propagation properties of an elastic medium. Actually, the visualization of the slowness surface is, in general, a nontrivial task. Indeed, for low-symmetry media, the left-hand side of the propagation condition cannot be factorized, which causes the slowness surface to be a complicated self-intersecting connected manifold. Then one may produce a 3-D plot showing, for each $\hat{\mathbf{k}}$, only the highest value of $\sqrt{s^2}$ (as, e.g., in Abbudi and Barnett, 1991, and Carcione and Cavallini, 1994); or, alternatively, draw 2-D plots of sections with successively inclined planes (Carcione and Cavallini, 1995). On the other hand, the axial and mirror symmetries of a transversely isotropic medium considerably simplify the problem, in that a single quadrant of a plane containing the axis is enough to describe the whole slowness surface. We shall now use the slowness surfaces of two transversely isotropic media and of their best isotropic approximations to show the effects of anisotropy on wave propagation.

Figures 5 and 6 show the slowness surfaces of the two shale samples with, respectively, the

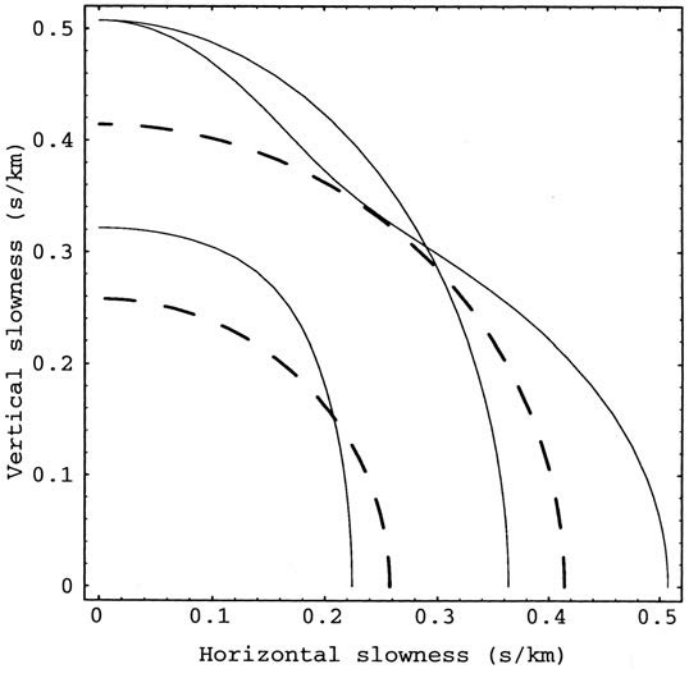

Fig. 6. - Slowness surfaces for the dry shale sample having the highest anisotropy index among the 44 such samples considered in Vernik and Liu (1997). Solid lines (—) represent the slowness surfaces of the sample assumed as transversely isotropic, while broken lines (- -) represent the slowness surfaces of the corresponding best isotropic approximation, which in this case turns out to be a very poor one.

minimum and maximum anisotropy index among the 44 samples considered above. It is clear that while in the former case the slowness surfaces of the best isotropic approximation almost coincide with the exact ones, in the latter the discrepancy is high.

4. Discussion and conclusions

We have computed the Lamé parameters of the best isotropic approximation of an anisotropic medium, using a new method that clarifies the geometric and physical contents of the resulting formulae.

Some of the results shown in this work may also be deduced from the theory presented in a classical article by Backus (1970). For example, our parameters λ_0 and μ_0 are related to Backus parameters H and h by $\lambda_0 = H + h$ and $\mu_0 = \mathrm{H} - h/2$. Using the expressions of H and h in terms of the stiffness tensor in Voigt notation (Backus, 1970, p. 662) yields our equations (27) and (28), provided that a misprint in Backus's article be corrected: the factor 1/18 in Backus's expression for P_{ij} (Backus, 1970, p. 663) should be changed into 1/9. However, it is to be noted that the present approach is much simpler, both conceptually and computationally, also because of its more limited scope. Moreover, the emphasis in Backus's article is on algebraic issues, as a canonical decomposition of the stiffness tensor, whereas the problem of approximation plays the major role here.

Our main results, namely equations (8) and (9) together with their versions in terms of coordinates, are useful whenever one wishes to ascertain how much more insight an anisotropic model has produced with respect to the best isotropic model. Consequently, applications may be envisaged in several fields. Measurements of anisotropy are performed on a routine basis in rock-physics laboratories nowadays. For example, shales (which are of great interest to exploration seismology) exhibit a substantially anisotropic behaviour (e.g., Schoenberg, 1996). Anisotropy plays an important role in earthquake seismology too (cf. the concise but thorough review by Kawasaki (1989)). Finally, anisotropy has to be taken into account in reservoir engineering as well, because stress-induced anisotropic effects greatly change the mechanical properties of porous rocks, where the application of a uniaxial stress partly closes the cracks, thus increasing the velocity of seismic waves along the symmetry axis (Bourbié et al., 1987).

Here we have seen a histogram of the anisotropy index of 44 dry shale samples, and the slowness surfaces of the least and the most anisotropic cases. This analysis shows that, as a rule, the isotropic approximation for shales is rather poor, and one has to resort to models containing more than two parameters, as the three-parameter ANNIE model (Schoenberg et al., 1989). Thus, an important (but challenging) problem now arises: that of finding three-parameter models of shales that are even better than ANNIE.

Acknowledgements. The author is grateful to Professor Anthony F. Gangi for helpful discussions and for kindly reading the first draft of the manuscript. Helpful remarks from two referees (M. Cara and J. Sileny) are also gratefully acknowledged.

Appendix 1 - Useful concepts and results from linear and tensor algebra

An introduction to linear algebra, with emphasis on the geometric interpretation of concepts and methods, may be found in the text book by Banchoff and Wermer (1991). This Appendix briefly summarizes the main concepts and results that are used in the main body of this paper.

Let X be a real finite-dimensional vector space with a scalar product. The set of all linear operators over X is denoted by $L[X]$. The expressions "operator" and "tensor (of order 2)" are often used as synonyms because of the natural isomorphism between the space of linear operators and that of bilinear forms. Moreover, "operator" is a synonym of "matrix" when X is the space of all real n-tuples.

The set $L[X]$ inherits the algebraic structure of linear space from X in an obvious way. We shall see, in a moment, that we may also define a scalar product in $L[X]$, and that this construction can be made in a natural (i.e., coordinate-free) way. But, first, we need to introduce the *trace* of a linear operator $\mathbf{A}$ (in symbols, trc[$\mathbf{A}$]), which may be defined as the sum of the eigenvalues of $\mathbf{A}$ counted with

their algebraic multiplicity. Then, the transpose $\mathbf{A}^T$ is the unique linear operator that satisfies the identity $\mathbf{x} \cdot \mathbf{A}^T \mathbf{y} = \mathbf{A}\mathbf{x} \cdot \mathbf{y}$. The scalar product in *L[X]* may now be defined through

$$\mathbf{A} \cdot \mathbf{B} = \mathrm{trc}\left[\mathbf{A}^T \circ \mathbf{B}\right] \qquad \text{for } \mathbf{A},\ \mathbf{B} \in L[X], \tag{49}$$

where the circle ($\circ$) denotes map composition. The notions of norm and orthogonality of operators then follow, as in the case of ordinary vectors. The symmetric part of **A** is defined by sym[**A**] = (1/2)(**A** +$\mathbf{A}^T$).

The orthogonal projection of a vector $\mathbf{x} \in X$ onto a subspace $S \subset X$ is the unique vector $\mathbf{x}_0 \in S$ orthogonal to $\mathbf{x} - \mathbf{x}_0$. One can also show that, among the vectors of *S*, the vector $\mathbf{x}_0$ is the closest to **x**: in other words, $\mathbf{x}_0$ is the best approximation of **x** that we can find in *S*.

Finally, we recall that the tensor product $\mathbf{u} \otimes \mathbf{v}$ of two vectors **u**, **v** in *X* is the linear operator over *X* such that $(\mathbf{u} \otimes \mathbf{v})\ \mathbf{x} = (\mathbf{v} \cdot \mathbf{x})\ \mathbf{u}$ for any vector **x** in *X*. Those who are familiar with quantum mechanics will recognize the tensor product as the product of a "ket" vector $|\mathbf{u}\rangle$ and a "bra" vector $\langle\mathbf{u}|$. A useful identity is $\mathrm{trc}[\mathbf{a} \otimes \mathbf{b}] = \mathbf{a} \cdot \mathbf{b}$.

Now, assume that **a** and **b** are two linearly independent, but possibly non orthogonal, vectors. Then, by using the Schmidt orthonormalization procedure, we can find two orthonormal vectors, $\hat{\mathbf{a}}$ and $\hat{\mathbf{b}}$, that are linear combinations of **a** and **b**. Thus, the orthogonal projector on span{**a**, **b**} (the subspace of all linear combinations of **a** and **b**) is given by $P = \hat{\mathbf{a}} \otimes \hat{\mathbf{a}} + \hat{\mathbf{b}} \otimes \hat{\mathbf{b}}$, which yields

$$P = \frac{1}{a^2 b^2 - (\mathbf{a} \cdot \mathbf{b})^2}\left(b^2 \mathbf{a} \otimes \mathbf{a} + a^2 \mathbf{b} \otimes \mathbf{b} - 2(\mathbf{a} \cdot \mathbf{b})\mathrm{sym}[\mathbf{a} \otimes \mathbf{b}]\right), \tag{50}$$

where, for brevity, we have put $a^2 = \| \mathbf{a} \|^2 = \mathbf{a} \cdot \mathbf{a}$. This last formula is used in Section 2.1 to obtain the main result of this paper.

Appendix 2 - Voigt's condensed notation from the point of view of abstract algebra

The aim of this appendix is to obtain Voigt's condensed notation using the methods of abstract algebra. The usefulness of this approach will be clarified in Appendix 3.

We call the following set of tensors *Voigt stress basis*:

$$\mathbf{V}_i^{stress} = \hat{\mathbf{E}}_i, \qquad \text{for } i = 1,\ 2,\ 3; \tag{51}$$

$$\mathbf{V}_I^{stress} = \sqrt{2}\hat{\mathbf{E}}_I, \qquad \text{for } i = 4,\ 5,\ 6; \tag{52}$$

We also call the following set of tensors Voigt strain basis:

$$\mathbf{V}_i^{strain} = \hat{\mathbf{E}}_i, \qquad \text{for } i = 1,\ 2,\ 3; \tag{53}$$

$$\mathbf{V}_I^{strain} = \left(1/\sqrt{2}\right)\hat{\mathbf{E}}_I, \qquad \text{for } i = 4,\ 5,\ 6; \tag{54}$$

Each of these sets of tensors constitutes a basis of L_s [$\Re^3$]; moreover, the following duality relationship holds:

$$\mathbf{V}_I^{strain} \cdot \mathbf{V}_J^{stress} = \delta_{IJ} \qquad \text{for} \quad I, J = 1,...,6 \tag{55}$$

Hence the stress S may be expanded as

$$\mathbf{S} = \sum_{I=1}^{6} S_I \mathbf{V}_I^{stress} = \sum_{i,j=1}^{3} \sigma_{ij} \hat{\mathbf{e}}_i \otimes \hat{\mathbf{e}}_j, \tag{56}$$

where $S_I = \mathbf{V}_I^{strain} \cdot \mathbf{S}, \quad \sigma_{ij} = \left(\hat{\mathbf{e}}_i \otimes \hat{\mathbf{e}}_j\right) \cdot \mathbf{S}$ and then

$$S_i = \sigma_{ij} \qquad \text{for} \quad \text{i} = 1,\ 2,\ 3, \quad S_4 = \sigma_{23}, \quad S_5 = \sigma_{13}, \quad S_6 = \sigma_{12}. \tag{57}$$

Likewise, the strain **E** may be expanded as

$$\mathbf{E} = \sum_{I=1}^{6} E_I \mathbf{V}_I^{strain} = \sum_{i,j=1}^{3} \in_{ij} \ \hat{\mathbf{e}}_i \otimes \hat{\mathbf{e}}_j, \tag{58}$$

where $E_1 = \mathbf{V}_I^{stress} \cdot \mathbf{E}, \quad \varepsilon_{ij} = \left(\hat{\mathbf{e}}_i \otimes \hat{\mathbf{e}}_j\right) \cdot \mathbf{E}$ and then

$$E_i = \in_{ii} \qquad \text{for} \quad \text{i} = 1,\ 2,\ 3, \quad E_4 = 2 \in_{23}, \quad E_5 = 2 \in_{13}, \quad E_6 = 2 \in_{12}. \tag{59}$$

Generalized Hooke's law may be written as **S** = *C*[**E**], where *C* is a linear operator. Hence equations (56) and (58) yield

$$\sigma_{ij} = \sum_{k,l=1}^{3} C_{ijkl} \ \varepsilon_{kl}, \qquad \text{where} \quad C_{ijkl} = \left(\hat{\mathbf{e}}_i \otimes \hat{\mathbf{e}}_j\right) \cdot C\left[\hat{\mathbf{e}}_k \otimes \hat{\mathbf{e}}_l\right]. \tag{60}$$

and

$$S_I = \sum_{J=1}^{6} c_{IJ} E_J, \qquad \text{where} \quad c_{IJ} = \mathbf{V}_I^{strain} \cdot C\left[\mathbf{V}_J^{strain}\right]. \tag{61}$$

The relationship between 2-index and 4-index components can be readily established. Indeed, defining the symmetric function *F* [*i, j*] as

$$F[i,i] = i \qquad i = 1,\ 2,\ 3, \quad F[1,2] = 6, \quad F[1,3] = 5, \quad F[2,3] = 4, \tag{62}$$

it is seen that

$$\mathbf{V}_{F[i,j]}^{strain} = \text{sym}\left[\hat{\mathbf{e}}_i \otimes \hat{\mathbf{e}}_j\right] \qquad \text{for} \ \ i = 1,\ 2,\ 3 \tag{63}$$

and then

$$C_{ijkl} = c_{F[i,j],F[k,l]} \qquad \text{for } i,\ j,\ k,\ l = 1,\ 2,\ 3. \tag{64}$$

Equations (56) - (64) are in agreement with Voigt's notation as presented, for example, in Mehrabadi and Cowin (1990). Thus, we have obtained the abbreviated subscript notation (see also Auld, 1990) in the general framework of linear algebra (by choosing suitable bases in appropriate spaces) and not just as an ad hoc trick for manipulating stress and strain components.

Appendix 3 - Pitfalls in the use of Voigt's condensed notation

Section 2 showed us that the trace of the stiffness operator is *not* equal to the trace of the matrix that represents it in Voigt notation (see eqns. (22) and (26)), and we were thus compelled to introduce a canonical basis as an intermediate step towards the computation of approximate Lamé parameters in Voigt notation. The aim of this appendix is to clarify the algebraic reasons for this discrepancy, and to point out that the same occurs for the other algebraic invariants, such as the determinant and the eigenvalues.

It is well known that a matrix that represents a linear operator (over a finite dimensional space) has the same eigenvalues and eigenvectors as the operator itself, provided that the *same* basis has been used to represent vectors both in the domain and in the range of the operator. But, if we choose *different* bases for the domain and the range, the eigenvalues of the operator and those of the matrix may differ. Consider the identity operator over the two-dimensional space of couples of real numbers, as an example. If we choose {{0, 1}, }{1, 0}} as a basis for its domain and {{0, 1}, }{2, 0}} as a basis for its range, then the identity operator is represented by the matrix

$$\begin{bmatrix} 1 & 0 \\ 0 & 1/2 \end{bmatrix},$$

which has a spurious eigenvalue 1/2. Of course, it is an awkward choice that of fixing one basis for the domain and another for the range, but this is actually the case for Voigt's condensed notation, where - as we have seen in Appendix B - the strain basis is used for the domain of the stiffness operator and the stress basis is used for its range.

As a conclusion, it is worthy of note that the eigenvalues and eigenvectors of the stiffness operator are not just a mathematical curiosity, but have an intrinsic physical interest, in that they lead to a simple formula for the strain energy (Thomson, 1856) and may be profitably used in formulating anisotropic viscoelastic rheologies (Carcione and Cavallini, 1994).

References

Abbudi M. and Barnett D. M.; 1991: *Three-dimensional computer visualization of the slowness surfaces of anisotropic crystals.* In: Wu J. J., Ting T. C. T., and Barnett D. M. (eds), Modern theory of anisotropic elasticity and applications. SIAM, Philadelphia, pp. 290-300.

Arts R. J.; 1993: *A study of general anisotropic elasticity in rocks by wave propagation: theoretical and experimental aspects.* Ph. D. Thesis, Université P. et M. Curie, Paris (France), 248 pp.

Auld B. A.; 1990: *Acoustic fields and waves in solids.* Vol. 1, 2.nd edition, Robert Krieger Publishing Co., Malabar (Florida), 435 pp.

Babuska V. and Cara M.; 1991: *Seismic anisotropy in the Earth*. Kluwer, Dordrecht, 217 pp.

Backus G.; 1970: *A geometrical picture of anisotropic elastic tensors*. Revs Geophys. Space Phys., **8**, 633-671.

Banchoff T. and Wermer J.; 1991: *Linear algebra through geometry.* 2.nd ed., Springer-Verlag, New York, 305 pp.

Bourbie T., Coussy O. and Zinsner B.; 1987: *Acoustics of porous media*. Editions Technip, Paris, 334 pp.

Carcione J. M.; 1992: *Anisotropic Q and velocity dispersion of finely layered media*. Geophys. Prospecting, **40**, 761-783.

Carcione J. M. and Cavallini F.; 1995: *Attenuation and quality factor surfaces in anisotropic -viscoelastic media.* Mech. of Mater, **19**, 311-327.

Carcione J. M. and Cavallini F.; 1994: *A rheological model for anelastic anisotropic media with applications to seismic wave propagation.* Geophys. J. Internat, **119**, 338-348.

Crampin S.; 1981: *A review of wave motion in anisotropic and cracked elastic media.* Wave Motion, **3**, 343-391.

Curie P.; 1884: *Sur la symétrie.* Bull. Soc. Mineral. France, **7**, 418-457.

Fedorov F. I.; 1968: *Theory of elastic waves in crystals.* Plenum Press, New York, 375 pp.

Fjær E., Holt R. M. and Rathore J. S. (eds); 1996: *Seismic anisotropy.* Society of Exploration Geophysics, Tulsa (Oklahoma), 763 pp.

Grant F. S. and West G. F.; 1965: *Interpretation theory in applied geophysics.* McGraw-Hill, New York, 583 pp.

Gurtin M. E.; 1981: *An introduction to continuum mechanics.* Academic Press, San Diego (California), 265 pp.

Helbig K.; 1994: *Foundations of anisotropy for exploration seismics.* Pergamon, Oxford, 486 pp.

Kawasaki I.; 1989: *Seismic anisotropy in the Earth.* In: James D. E. (ed), The encyclopedia of solid Earth geophysics, Van Nostrand Reinhold, New York, 1328 pp.

Mehrabadi M. M. and Cowin S. C.; 1990: *Eigentensors of linear anisotropic elastic materials.* Q. Jl. Mech. & Appl. Math., **43**, 15-41.

Schoenberg M., Muir F. and Sayers C.; 1996: *Introducing ANNIE: a simple three-parameter anisotropic velocity model for shales.* J. Seismic Explor., **5**, 35-49.

Thill R. E., Bur T. R. and Steckley R. C.; 1973: *Velocity anisotropy in dry and saturated rock spheres and its relation to rock fabric.* Int. J. Rock Mech. Min. Sci. and Geomech. Abstr., **10**, 535-557.

Thomsen L.; 1986: *Weak elastic anisotropy.* Geophysics, **51**, 1954-1966.

Thomson W. (Lord Kelvin); 1856: *Elements of a mathematical theory of elasticity.* Phil. Trans. R. Soc., **166**, 481-498.

Vernik L. and Liu X.; 1997: *Velocity anisotropy in shales: A petrophysical study*. Geophysics, **62**, 521-532.